A Method to Reduce Small-Angle Scattering in Monte Carlo Device Analysis

Hans Kosina, *Member, IEEE*

***Abstract*—Ionized-impurity scattering is an anisotropic process showing a high preference for small scattering angles. In a Monte Carlo simulation of a semiconductor device many small-angle scattering events have to be processed, although the contribution of these events to carrier momentum relaxation is small. A new method is presented which reduces the amount of small-angle scattering very effectively. In the simulation an isotropic process is used which yields the same momentum relaxation time as the anisotropic process. A theoretical analysis based on the Boltzmann equation is carried out. Monte Carlo calculations are performed over a wide range of doping concentrations, lattice temperatures and electric fields. No systematic difference is found in the results from the anisotropic and the isotropic scattering models. For a given accuracy, the reduction of needed scattering events and free flights can be more than one order of magnitude at low and medium doping concentrations.**

I. Introduction

TO simulate carrier transport in submicrometer-scale semiconductor devices the Monte Carlo technique has found wide spread application [1]–[4]. Due to high doping concentrations in such devices carrier mobility is considerably reduced by ionized-impurity scattering.

The large range of Coulomb forces makes the scattering cross section of a single ion very large, or even infinite if no screening is assumed. Therefore, Coulomb scattering is a strongly anisotropic process with a high probability for small-angle scattering events. Although these events occur frequently, their effect on momentum relaxation is small. This property of Coulomb scattering, though being physically sound, imposes several problems upon the Monte Carlo technique. A great many of small-angle scattering events have to be processed consuming computation time. Very short free-flight times are obtained which further degrade the efficiency of the Monte Carlo procedure.

Fig. 1 illustrates this problem. As an example, the low-field electron mobility as a function of the ionized-impurity concentration has been calculated using the Monte Carlo method. The upper curve shows that even at low impurity concentrations more than 90% of all scattering events are of Coulomb type. Phonon scattering constitutes the rest. At low impurity concentrations we observe the paradoxical situation that on the one hand ionized-impurity scattering is the most frequent process, and that, on the other hand, it has nearly no effect on the mobility. This discrepancy occurs because the collisional and the momentum cross sections for the considered process can differ by several orders of magnitude.

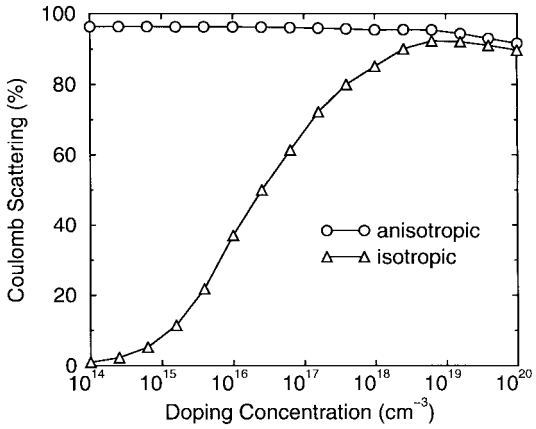

Fig. 1. Relative frequency of Coulomb scattering as a function of doping concentration. Because of the large range of Coulomb forces the frequency is very high even at low concentrations (◯). The isotropic scattering model reduces the relative frequency effectively, especially at low concentrations (△). Conditions are $T = 300$ K and $E = 700$ V/cm.

In the following a method is presented which allows to reduce the amount of small-angle scattering very efficiently while the underlying transport problem remains virtually unchanged. Instead of using the highly anisotropic scattering cross section of screened Coulomb interaction an equivalent cross section is used, which is isotropic, and yields the same the momentum relaxation time as the anisotropic cross section.

II. Theory

A. Scattering Cross Section

Anisotropic, elastic scattering can be discussed in terms of the differential scattering cross section, $\sigma(k, \cos\theta)$. For a given wave number k, the differential scattering cross section can be interpreted as a probability density function of the scattering angle, θ.

Scattering of charge carriers is a quantum mechanical process for which a transition probability $P(\mathbf{k}, \mathbf{k}')$ between the states $\mathbf{k}$ and $\mathbf{k}'$ can be derived. Due to symmetry of the scattering potential, P depends only on θ, the angle between $\mathbf{k}$ and $\mathbf{k}'$, and not on the azimuthal angle φ. In the following the notation $z = \cos\theta$ is adopted. For ionized-impurity scattering the differential scattering cross section σ and the quantum

Manuscript received May 19, 1998; revised January 19, 1999. The review of this paper was arranged by Editor A. H. Marshak.

The author is with the Institute for Microelectronics, Vienna A-1040, Austria.

Publisher Item Identifier S 0018-9383(99)04598-0.

mechanical transition probability P are related by (see, e.g., [5])

$$\sigma(k,z) = \frac{1}{N_I v_g(k)} \cdot \frac{V_0}{(2\pi)^3} \int_0^\infty P(k,k',z) k'^2 \, dk'. \quad (1)$$

N_I denotes the concentration of the impurity centers, V_0 is the volume of the crystal, and v_g is the electron group velocity which is assumed to be derived from an isotropic band structure, $v_g = \partial E / \partial \hbar k$. From the differential scattering cross section the total scattering rate λ and the momentum relaxation time τ_m can be obtained by integration.

$$\lambda(k) = 2\pi N_I v_g(k) \int_{-1}^{1} \sigma(k,z) \, dz \quad (2)$$

$$\frac{1}{\tau_m(k)} = 2\pi N_I v_g(k) \int_{-1}^{1} (1-z)\sigma(k,z) \, dz. \quad (3)$$

To tackle the problem of small-angle scattering we construct an equivalent scattering cross section $\tilde{\sigma}$ that fulfills two requirements.

1) The equivalent cross section is isotropic

$$\frac{\partial \tilde{\sigma}(k,z)}{\partial z} \equiv 0. \quad (4)$$

2) The momentum relaxation times of the equivalent and the original cross section are identical

$$\tilde{\tau}_m(k) \equiv \tau_m(k). \quad (5)$$

B. Carrier Mobility

For an arbitrary nonequilibrium distribution function f the mobility is defined as [4]

$$\mu = \frac{e}{\hbar} \cdot \frac{\left| \int \mathbf{v}_g(\mathbf{k}) f(\mathbf{k}) \, d\mathbf{k} \right|}{\left| \int \mathbf{k} \tau_m^{-1}(\mathbf{k}) f(\mathbf{k}) \, d\mathbf{k} \right|}. \quad (6)$$

With (5) it is ensured that the main transport parameter, namely the nonequilibrium mobility (6), is not altered as long as the distribution function remains unchanged.

Combining (2), (3) and (4), (5) the scattering cross section $\tilde{\sigma}$ and the total scattering rate $\tilde{\lambda}$ of the equivalent model can readily be obtained.

$$\tilde{\sigma}(k,z) \equiv \tilde{\sigma}(k) = \frac{1}{2} \int_{-1}^{1} (1-z')\sigma(k,z') \, dz' \quad (7)$$

$$\tilde{\lambda}(k) = \frac{1}{\tau_m(k)}. \quad (8)$$

For an anisotropic scattering process with a high preference for forward-scattering the momentum relaxation rate τ_m^{-1} is always smaller than the total scattering rate λ. Therefore, using the equivalent scattering rate (8) in a Monte Carlo procedure has the advantage that ionized-impurity scattering becomes a less frequent scattering process. The effect, that the equivalent scattering model requires a considerable lower number of Coulomb scattering events to be processed, can be interpreted as a gathering of many scattering events each with small momentum transfer to one scattering event with large momentum transfer.

C. Boltzmann Equation

Now we investigate the question how the usage of the equivalent scattering model affects the considered transport problem. For this purpose we analyze the scattering integral of the Boltzmann transport equation for the nondegenerate case

$$\left(\frac{\partial f}{\partial t} \right)_c = \frac{V_0}{(2\pi)^3} \int P(\mathbf{k}', \mathbf{k}) f(\mathbf{k}') \, d\mathbf{k}' - \lambda(\mathbf{k}) f(\mathbf{k}). \quad (9)$$

The transition probability P is assumed to obey Fermi's golden rule

$$P(\mathbf{k}, \mathbf{k}') = \frac{2\pi}{\hbar} |M(\mathbf{q})|^2 \delta(E - E') \quad (10)$$

where M denotes the interaction matrix element. To the equivalent isotropic scattering model some artificial matrix element $\tilde{M}$ can be assigned, given by an angular average.

$$\tilde{M}^2(k) = \frac{1}{2} \int_{-1}^{1} (1-z) M^2(q(k,z)) \, dz. \quad (11)$$

For an elastic scattering mechanism as considered here the momentum transfer equals $q^2(k,z) = 2k^2(1-z)$. Using (11) the scattering integral evaluates to

$$\widetilde{\left(\frac{\partial f}{\partial t} \right)}_c = -\frac{f_A(\mathbf{k})}{\tau_m(k)} \quad (12)$$

with f_A denoting the antisymmetric part of the distribution function.

For the anisotropic process we evaluate the scattering integral by making an assumption on the shape of the distribution function, which is usually referred to as diffusion approximation

$$f(k, \cos\theta) = f_S(k) + f_1(k) \cos\theta. \quad (13)$$

Integration again filters out the antisymmetric part of the distribution function

$$\left(\frac{\partial f}{\partial t} \right)_c = -\frac{f_1(k) \cos\theta}{\tau_m(k)}. \quad (14)$$

Comparison of (12) and (14) shows that the scattering integral, and hence the Boltzmann equation, will not change if the anisotropic part of the distribution function is of the form $f_A(\mathbf{k}) = f_1(k) \cos\theta$.

The impact of this restriction is discussed in the following. Coulomb scattering plays an important role especially at low electric fields, where the approximation (13) is certainly very accurate. At high fields, however, where it might become necessary to include higher powers of $\cos\theta$ in (13), the influence of Coulomb scattering diminishes rapidly. For example, the saturation velocity does not depend on the doping concentration and hence not on impurity scattering. Furthermore, one should keep in mind that λ and P in the scattering term (9) comprises contributions of many scattering processes. If the shape of distribution function deviates from (13), then only the contribution of Coulomb scattering to the scattering integral is modified to some degree, while the contributions of all other processes remain unchanged. Hence, we conclude that at higher temperatures, when the

phonon processes dominate, the isotropic treatment of impurity scattering works well, and that significant errors might be introduced if the temperature gets very low.

III. The Ionized Impurity Scattering Model

In the computer experiments presented in the next section we employ the ionized impurity scattering model described in [6]. In this section we repeat the main equations of the model and explain some implementation details. The Fourier transform of the scattering potential is given by

$$|V(q)|^2 = \left(\frac{Ze}{\epsilon_0\epsilon_r}\right)^2 \frac{1}{\left(q^2+\beta_s^2 G(q)\right)^2}\left(1+\frac{\sin qR}{qR}\right) \quad (15)$$

where β_s denotes the inverse Fermi–Thomas screening length, G is the screening function, and R is the average distance between ions defined as $R = (2\pi N_I)^{-1/3}$. The scattering potential (15) accounts for momentum-dependent screening and a correction term for coherent multi-ion scattering.

With G being approximated by a rational function [6], the total scattering rate can, in principle, be obtained from (15) by analytical integration. Due to the complexity of the result it is more efficient both in terms of implementation effort and computation time requirement to use an internal self-scattering scheme.

An upper bound for (15) in the interval $q \in [0, 2k]$ is, for example, given by

$$|V(q)|^2 \le \left(\frac{Ze}{\epsilon_0\epsilon_r}\right)^2 \frac{2}{\left(q^2+\beta_1^2\right)^2} = 2|V_{\mathrm{BH}}(q)|^2$$
$$\beta_1^2 = \beta_s^2 G(2k). \quad (16)$$

Since G is a monotonically decreasing function it is evaluated at $q_{\max} = 2k$ to obtain a lower bound for the denominator. The potential at the right hand side of (16) is of the form of the Brooks–Herring potential, however, with a different screening parameter β_1. With the Brooks–Herring potential the required q-integrations are straight-forward, and one obtains upper bounds for the physical scattering rate λ and the physical momentum relaxation rate $\tilde{\lambda}$:

$$\lambda(k) \le 2\lambda_{\mathrm{BH}}(k)$$
$$\tilde{\lambda}(k) \le 2\tilde{\lambda}_{\mathrm{BH}}(k).$$

The upper bounds are

$$\lambda_{\mathrm{BH}}(k) = C(k)\cdot\frac{1}{2\beta_1^2}\cdot\frac{b}{1+b} \quad (17)$$

$$\tilde{\lambda}_{\mathrm{BH}}(k) = C(k)\cdot\frac{1}{4k^2}\cdot\left(\ln(1+b)-\frac{b}{1+b}\right). \quad (18)$$

In these equations we have set $b = 4k^2/\beta_1^2$, and the energy-dependent pre-factor C is of the form

$$C(k) = \frac{N_I Z^2 e^4}{2\pi\hbar^2(\epsilon_0\epsilon_r)^2 v_g(k)}. \quad (19)$$

Note that both $\tilde{\lambda}_{\mathrm{BH}}$ and $\tilde{\lambda}$ are rates of isotropic scattering processes. In a Monte Carlo procedure, for the free flight time calculation and the selection of the scattering process the rate $2\tilde{\lambda}_{\mathrm{BH}}$ is used. Now there is a well-defined probability P of accepting a selected Coulomb scattering event $P = \tilde{\lambda}/2\tilde{\lambda}_{\mathrm{BH}}$. This probability can also be expressed as

$$P = \frac{\int_0^{2k}|V(q)|^2 q^3\,dq}{2\int_0^{2k}|V_{\mathrm{BH}}(q)|^2 q^3\,dq}. \quad (20)$$

Instead of solving these integrals directly one can think of solving them by means of Monte Carlo integration. Then the internal self-scattering algorithm can be defined as follows. A random number $q_r \in [0, 2k]$ is chosen according to the probability density function $|V_{\mathrm{BH}}(q)|^2 q^3$. Then a random number p_r is chosen evenly distributed between 0 and $2|V_{\mathrm{BH}}(q_r)|^2$. If $p_r < |V(q_r)|^2$ then the scattering event is accepted, otherwise it is rejected and self-scattering is performed instead.

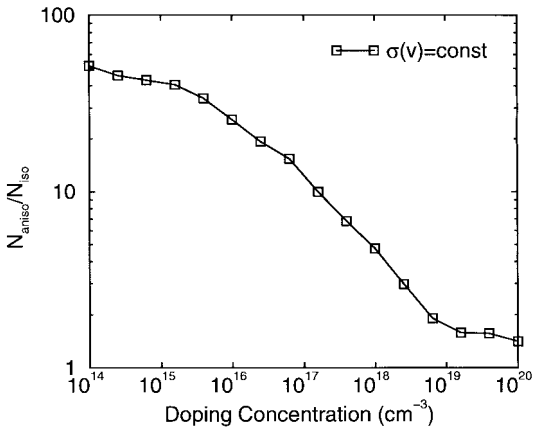

Fig. 2. N_{aniso} and N_{iso} are the numbers of free flights and scattering events that have to be processed when using the anisotropic and isotropic scattering models, respectively, in order to achieve the same statistical uncertainty of the mean velocity. The ratio of both numbers corresponds to the saving in computation time. Conditions are $T = 300$ K and $E = 700$ V/cm.

IV. Results and Discussion

Transport calculations in uncompensated silicon are performed. In addition to ionized-impurity scattering the transport model comprises acoustic intra-valley scattering and six different types of inter-valley phonon scattering [7]. We adopt a nonparabolic and isotropic band structure using an effective mass of $m^* = 0.32$ and a nonparabolicity coefficient of $\alpha = 0.5$ eV^{-1}.

In Fig. 1 the relative frequencies of anisotropic and isotropic Coulomb scattering are plotted. Especially at low doping concentrations, the isotropic scattering model yields a considerably reduced Coulomb scattering frequency. To estimate the gain in computation time quantitatively, we plot in Fig. 2 the number of processed scattering events due to the anisotropic model over the number of processed events due to the isotropic model. For both simulations the statistical uncertainty of the drift velocity v, measured by the standard deviation, $\sigma(v)$, is equal. The standard deviation is calculated by the method reported in [7].

If a Monte Carlo algorithm is considered for which the effort for processing one free-flight is independent from its duration, then the ratio plotted in Fig. 2 directly gives the saving in

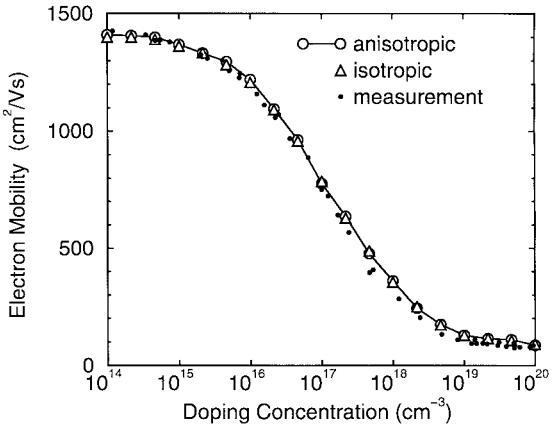

Fig. 3. Calculated low-field mobility at 300 K in comparison with experimental data [8]. The isotropic and the anisotropic scattering model yield the same results.

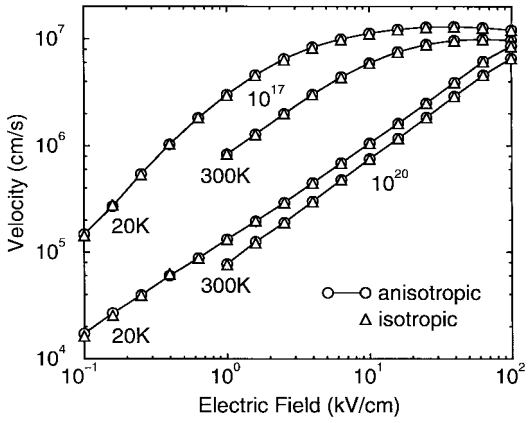

Fig. 5. Mean velocity as function of the electric field for two doping levels at 20 and 300 K. Even in the high field region the isotropic scattering model performs very well.

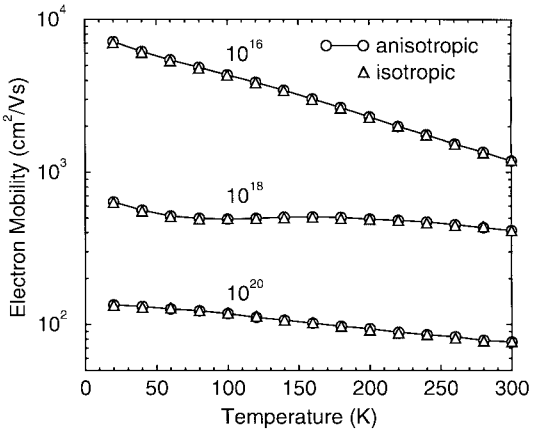

Fig. 4. Low-field mobility ($E = 1$ kV/cm) as function of the lattice temperature with the doping concentration (in units of cm^{-3}) as parameter. No systematic differences can be observed between the results from the isotropic and anisotropic scattering models.

computation time. The computation time reduction is about 50 at $N_I = 10^{14}$ cm^{-3} and is still one order of magnitude at $N_I = 10^{17}$ cm^{-3}. At very high concentrations the gain is on the order of a few 10%.

Fig. 3 shows the low-field mobility calculated with the anisotropic and the isotropic scattering models in comparison with experimental data [8]. The full model described in [6] is used, including the second Born correction, plasmon scattering, and the Pauli exclusion principle. No systematic difference in the simulated data is found, even not at very high doping concentrations where momentum relaxation is dominated by ionized impurity scattering.

In Section II, we pointed out that the isotropic scattering model may become inaccurate if the distribution function in not well represented by the diffusion approximation. Since there is no theoretical estimate for the possible error we performed simulations over a wide range of lattice temperatures and electric fields. The results in Figs. 4 and 5 indicate that the isotropic model does not cause any systematic deviation within the considered parameter ranges. In these two computer experiments both plasmon scattering and the Pauli principle were neglected in order to keep the transport problem linear.

V. Problems at Low Energies

Finally we discuss the peculiar energy-dependence of Coulomb scattering and propose a solution to the related problems. Characteristic of the Coulomb scattering rate is a peak at very low energies. This maximum is located at $E_\beta/4$, with $E_\beta = \hbar^2\beta_s^2/2m^*$, and increases with decreasing carrier concentration. For instance, at $N_I = 10^{16}$ cm^{-3} we have $E_\beta/4 \cong 0.02$ meV. This peak, which is due to the long range of the screened Coulomb interaction, appears both in the anisotropic and the equivalent isotropic scattering rates. The extraordinarily high scattering frequency at very low energies degrades the performance of a Monte Carlo simulation.

This problem can be avoided by using the statistical screening model introduced by Ridley [9]. In a form suited for Monte Carlo calculations [10] this model has become very popular. Statistical screening modifies the scattering cross section of the Brooks–Herring model as follows:

$$\sigma_{\mathrm{mod}}(k,z) = \sigma_{\mathrm{BH}}(k,z)\exp(-RN_I\pi b^2(z)). \qquad (21)$$

R denotes the average distance between the ions, and b is the impact parameter as function of the scattering angle. In this model the long-range part of the screened Coulomb interaction is cut off by the additional statistical screening mechanism. As a consequence the amount of small-angle scattering is effectively reduced, and a scattering rate which behaves well at low energies is obtained

$$\lambda_{\mathrm{mod}}(k) = \frac{v_g(k)}{R}\left(1 - \exp\left(-\lambda_{\mathrm{BH}}(k)\frac{R}{v_g(k)}\right)\right). \qquad (22)$$

However, statistical screening is introduced somewhat ad hoc and is lacking any quantum mechanical basis. Our simulations show that statistical screening increases the low-field mobility for medium doping concentrations by 10% at 300 K and by 15% at 77 K, compared with the Brooks–Herring model. Therefore, the poor agreement of the Brooks–Herring model, which overestimates the mobility, even gets worse by adding statistical screening.

As an alternative, we introduce some empirical modification of the scattering rate. However, the influence of this

modification on the result can be controlled by a free parameter and can thus be kept below some desired limit.

To cut off the peak at some $\tilde{\lambda}_{\max}$, amongst others the harmonic mean can be used

$$\frac{1}{\tilde{\lambda}_{\mathrm{mod}}} = \frac{1}{\tilde{\lambda}} + \frac{1}{\tilde{\lambda}_{\max}}. \tag{23}$$

We choose $\tilde{\lambda}_{\max}$ to be proportional to the rate at which an electron traveling with group velocity v_g is crossing the radius of a screening-sphere β_s^{-1}

$$\tilde{\lambda}_{\max}(k, N_I) = W v_g(k) \beta_s(N_I). \tag{24}$$

W is a free parameter. For example, relative to the plain Brooks–Herring model the increase in low-field mobility at room temperature is below 1.5% for $W = 10$ and below 2.3% for $W = 5$.

VI. Conclusion

A method has been presented which effectively reduces the amount of small-angle scattering events that have to be processed in the course of a Monte Carlo transport calculation. The inverse momentum relaxation time for ionized-impurity scattering serves as scattering rate for an equivalent scattering process. The equivalent process, which is isotropic, exhibits an up to four orders of magnitude lower scattering rate, depending on doping concentration and carrier energy. An analysis of the scattering term of the Boltzmann transport equation indicates that using the equivalent, isotropic process rather than the anisotropic one has negligible influence on the transport problem of charge carriers in semiconductors, unless the temperature is very low. Monte Carlo calculations over a wide range of doping concentrations, lattice temperatures, and electric fields demonstrate the equivalence of the isotropic scattering model empirically. For a given accuracy, the reduction of computation time can more than one order of magnitude at low and medium doping concentrations. At very high concentrations the gain drops to a few 10%. To deal with the peak in the scattering rate at low energies an empirical modification of the scattering rate is presented whose effect on the mobility can be controlled by a free parameter.

Acknowledgment

The author would like to thank G. Kaiblinger-Grujin for many fruitful discussions, and S. Selberherr for continued encouragement.

References

[1] M. Fischetti and S. Laux, "Monte Carlo analysis of electron transport in small semiconductor devices including band-structure and space-charge effects," *Phys. Rev. B*, vol. 38, no. 14, pp. 9721–9745, 1988.

[2] J. Higman, K. Hess, C. Hwang, and R. Dutton, "Coupled Monte Carlo—Drift diffusion analysis of hot-electron effects in MOSFET's," *IEEE Trans. Electron Devices*, vol. 36, pp. 930–937, May 1989.

[3] F. Venturi, R. Smith, E. Sangiorgi, M. Pinto, and B. Riccó, "A general purpose device simulator coupling Poisson and Monte Carlo transport with applications to deep submicron MOSFET's," *IEEE Trans. Computer-Aided Design*, vol. 8, pp. 360–369, Apr. 1989.

[4] H. Kosina and S. Selberherr, "A hybrid device simulator that combines Monte Carlo and drift-diffusion analysis," *IEEE Trans. Computer-Aided Design*, vol. 13, pp. 201–210, Feb. 1994.

[5] D. Chattopadhyay and H. Queisser, "Electron scattering by ionized impurities in semiconductors," *Rev. Mod. Phys.*, vol. 53, pp. 745–768, Oct. 1981.

[6] H. Kosina and G. Kaiblinger-Grujin, "Ionized-impurity scattering of majority electrons in silicon," *Solid-State Electron.*, vol. 42, no. 3, pp. 331–338, 1998.

[7] C. Jacoboni and L. Reggiani, "The Monte Carlo method for the solution of charge transport in semiconductors with applications to covalent materials," *Rev. Mod. Phys.*, vol. 55, pp. 645–705, July 1983.

[8] G. Masetti, M. Severi, and S. Solmi, "Modeling of carrier mobility against carrier concentration in arsenic-, phosphorus- and boron-doped silicon," *IEEE Trans. Electron Devices*, vol. ED-30, pp. 764–769, July 1983.

[9] B. Ridley, "Reconciliation of the Conwell-Weisskopf and Brooks–Herring formulae for charged-impurity scattering in semiconductors: Third-body interference," *J. Phys. C: Solid State Phys.*, vol. 10, pp. 1589–1593, 1977.

[10] T. Van de Roer and F. Widdershoven, "Ionized impurity scattering in Monte Carlo calculations," *J. Appl. Phys.*, vol. 59, pp. 813–815, Feb. 1986.

Hans Kosina (S'88–M'92) was born in Haidershofen, Austria, in 1961. He received the Dipl.-Ing. degree in electrical engineering and the Ph.D. degree from the Vienna University of Technology, Vienna, Austria, in 1987 and 1992, respectively. In March 1998, he received the "venia docendi" on "Microelectronics."

For one year, he was with the Institute for Flexible Automation. In 1988, he joined the Institute for Microelectronics, the Vienna University of Technology, where he is currently an Associate Professor. His current interests include modeling of carrier transport and quantum effects in semiconductor devices, and computer-aided engineering in VLSI technology.